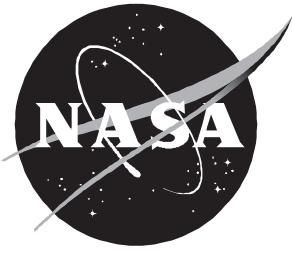


Galactic and Solar Cosmic Ray Shielding in Deep Space

John W. Wilson, Francis A. Cucinotta, H. Tai, Lisa C. Simonsen, Judy L. Shinn, Shelia A. Thibeault, and M. Y. Kim



Galactic and Solar Cosmic Ray Shielding in Deep Space

John W. Wilson, Francis A. Cucinotta, H. Tai, Lisa C. Simonsen, Judy L. Shinn, Shelia A. Thibeault, and M. Y. Kim

Langley Research Center • Hampton, Virginia

Available electronically at the following URL address: <http://techreports.larc.nasa.gov/ltrs/ltrs.html>

Printed copies available from the following:

NASA Center for AeroSpace Information
800 Elkridge Landing Road
Linthicum Heights, MD 21090-2934
(301) 621-0390

National Technical Information Service (NTIS)
5285 Port Royal Road
Springfield, VA 22161-2171
(703) 487-4650

Abstract

An analysis of the radiation hazards in support of NASA deep space exploration activities is presented. The emphasis is on materials required for radiation protection shielding. Aluminum has been found to be a poor shield material when dose equivalent is used with exposure limits for low Earth orbit (LEO) as a guide for shield requirements. Because the radiation issues are cost related—the parasitic shield mass has high launch costs—the use of aluminum as a basic construction material is clearly not cost-effective and alternate materials need to be developed. In this context, polyethylene is examined as a potentially useful material and demonstrates important advantages as an alternative to aluminum construction. Although polyethylene is useful as a shield material, it may not meet other design criteria (strength, stability, thermal); other polymer materials must be examined.

Introduction

The long-range strategic outlook for the “Human Exploration and Development of Space Enterprise” is to “[o]pen the space frontier to international human expansion and commercial development.” In order to accomplish these ends, “We look to the Space Technology Enterprise (STE) to develop revolutionary advanced technologies critical to establishing a sustained human presence in space” (ref. 1).

“The Enterprise works in partnership with the science community to create new scientific knowledge by studying the effects of gravity and the space environment on important biological, chemical and physical processes” (ref. 1). The hazards of space radiations are a primary limiting factor in future human space operations; hence, shielding technology is a critical design issue.

Within a few years of the discovery of particles of high charge and energy (HZE) as components of the galactic cosmic rays (GCR), the unique pattern of energy deposition on the microscopic scale raised issues with respect to effects on living cells (ref. 2). Although radiobiological knowledge has greatly improved, our ability to estimate risk to the astronaut from such exposures is still quite uncertain (ref. 3). No exposure limitation has been recommended for deep space missions as yet, but in the interim the recommendation is that estimates of interplanetary exposure using quality factors dependent on the linear energy transfer (LET) with exposure limits recommended for operations in low Earth orbit (LEO) be taken as a guide to deep space mission shield requirements. These LEO exposure limits were established under the assumption that the GCR components are diminished in LEO by their deflection in the Earth’s magnetic field so that LEO exposures are dominated by trapped protons and electrons. Deep space exposure estimates using LET-dependent quality factors result in exposures of as much as 1 Sv/yr near solar minimum depending on shielding. A large potential impact exists on the career of a space worker for whom annual expo-

sure limits (table 1) are currently 0.5 Sv/yr for the LEO environment with additional total career exposure limits that depend on age and gender (ref. 4). The primary limiting factor in future deep space manned operations is anticipated to be the health risks associated with exposures to galactic cosmic rays.

The galactic cosmic rays consist of all the known ions extending to very high energies with time variable intensities over the solar cycle exhibiting periodic maxima and minima in intensity with a variable 10- to 13-year cycle. The annual fluence for the main components are shown in figure 1 for the 1977 solar minimum and the 1981 solar maximum (ref. 5). The environmental data in the figure span the range of variation induced by the solar cycle in the GCR intensities as yet observed. The near-term deep space exploration objectives are contingent on current cost and emphasize the possibility of a low cost return to the Moon or going to Mars. Radiation protection systems (shielding, monitoring, and medical supplies) impact mission cost, and uncertainty in past shielding databases is inadequate for present design studies. For example, the required shielding to reduce the 5-cm-depth dose from GCR at solar minimum to 45 cSv behind an aluminum shield was estimated to be 2 g/cm² by the NCRP in 1989 (ref. 4), to be 7 g/cm² by Simonsen, Nealy, and Townsend in 1992 (ref. 6), and to be 55 ± 10 g/cm² by the present estimate (table 2) using current transport codes and databases. Whereas aluminum was considered a useful shield material a few years ago, now it is considered as not only a poor shield material but may even be hazardous to the astronaut’s health because dose equivalent may be a poor predictor of astronaut risk (ref. 7). The relative advantage of polymeric materials can be judged from table 2 in that only 17 g/cm² of polyethylene is required for a reduction in shield mass of approximately a factor of 3.

As an aid to understanding these recent developments in shield design technologies, the progression of aluminum shield GCR attenuation characteristics (refs. 8

through 13) is shown in figure 2. The lower curve is that generated by the code of Letaw, Silberberg, and Tsao (ref. 8) and used by the NCRP (ref. 4). The NUCFRG1 curve used the first Langley nuclear fragmentation database (ref. 9) and the corresponding first version space radiation transport code (ref. 10). Limiting values of the fragmentation cross sections for the primary ions can be made with the assumption of conservation of mass and charge in the event (unitary condition). The peripheral limit and central limit curves are those unitary limits on the projectile fragmentation which assure charge and mass conservation in breakup of the cosmic ions, not including the direct target knockout contributions to the transmitted fluence (ref. 11). The NUCFRG2 curve is from the revised NUCFRG1 database as a result of the experiments at 600 A MeV in the Bevalac facility (refs. 12 and 13). The two upper curves (labeled "Hard spectrum" and "Soft spectrum") include improved nuclear data for the knockout of light fragments from projectile and target nuclei and the uncertainty in their production spectra (ref. 14) and encompass our best current estimate of the attenuation of dose equivalent in aluminum. Clearly large changes in the nuclear data and transport procedures have occurred in the last several years. Only the completion of the transport code with the as yet neglected radiation components with added laboratory and flight validation will allow a final evaluation of the expected astronaut exposure. The remaining problem is relating the exposure fields at specific tissue sites within the astronaut to the tissue response and the related health risk.

Clearly, aluminum which was taken as a reasonable shield material a few years ago is now considered a poor candidate for future spacecraft construction. Indeed, the thickness of 55 g/cm² would make the deep space exploration cost very high (ref. 15); therefore, alternative materials must be examined to control the mission cost. Polymers (table 2) and polymer/composites (ref. 7) are among the alternate materials under consideration. In the present report, results are reviewed for the attenuation characteristics of aluminum and polyethylene as a potential shield material.

Radiation Environment and Computational Models

The model of Badhwar and O'Neill (ref. 5) is used to estimate the GCR environmental components. The model is represented by particle spectra for successive solar maxima and minima associated with solar cycles 19 through 22. The maximum observed GCR flux was near the 1977 solar cycle minimum at the end of cycle 21 and the highest GCR flux of the solar cycle maxima was observed during the peak solar activity in 1970. To establish a permanent human presence in space, one must

design for the maximum environmental intensity. In principle, one could conduct a mission near solar maximum to reduce exposure but the long-range prediction of when the solar cycle maximum will occur is poor and once it is missed another will not appear for 10 to 13 yr. In addition, in years of elevated solar activity, the possibility of a large solar particle event exists in which the annual exposure limit could be exceeded in several hours. Both the 1977 solar minimum and 1970 solar maximum environments are used to examine shielding requirements. The exposures for these environments in aluminum and polyethylene are shown in tables 2 and 3. The largest solar event observed in terms of the exposure potential to astronauts was the event on August 4, 1972 (fig. 3), which corresponds to approximately the 97 percentile annual solar particle fluence. An even larger event may occur with an estimated 3 percent probability.

In an actual engineering design study, we would model a baseline configuration of spacecraft and/or habitat to determine the geometric distribution of materials provided by the basic structure, internal and external equipment, consumables (ref. 16). Those results combined with the transport properties of the specific materials provide an estimate of the radiation environment in the spacecraft and/or habitat. Various configurations would be tried to improve the protection and minimize the mass of the construction. The choice of construction materials strongly influences the results as shown later. In such studies, many design requirements exist and one must evaluate the overall structural and thermal integrity of the design, the equipment requirements with power generation and distribution, as well as other environmental design criteria such as cabin air quality, flammability, and toxicity. Change in scenarios and alteration of mission objectives and mission operating plans would be used as trade-offs for the most efficient means of accomplishing the primary mission goals. Then the optimum placement of equipment to minimize parasitic shield requirements can be investigated. Obviously, efficient computational procedures are a base requirement for such design studies and the Langley code HZETRN has been proven to meet this requirement.

In the present study, simple spacecraft geometry is chosen in which an astronaut is assumed to be at the center of a large spherical shell of uniform material. The total shield mass is then proportional to the shield thickness in units of areal density. The geometry of the astronaut is represented by the Computerized Anatomical Model (CAM) containing 2400 separate geometric tissue regions of several different elemental compositions and densities (ref. 17). The emphasis is on the effectiveness of the shield material used in the construction of a spherical shell shield.

Currently large uncertainties exist in biological response, spacecraft shielding properties, and transport properties of body tissues to HZE particles, such as those which comprise the galactic cosmic rays. These uncertainties can be judged by the evolving changes in the transmission characteristics of aluminum shielding shown in figure 2. The uncertainty in astronaut risk to HZE particles consists of the biological response with uncertainties up to a factor of ≈ 5 , and to the transport properties of materials with uncertainties up to a factor of ≈ 2 . (See fig. 2.) Of little importance is the uncertainty in the GCR background environment which is estimated to be about 10 to 15 percent in the near-Earth environment. Long-range predictions are not yet possible, and the understanding of the near-Mars environment is limited. The anomalous cosmic ray components which are not represented in the present model mainly affect the dose and dose equivalent to the skin and ocular lens for very low shielding (few millimeters) and are of no practical consequence in the present study.

The HZETRN code is used to evaluate the transport of the primary ions into the spacecraft interior. Given the interior environment, the transport through the astronaut tissues in reaching critical tissues is evaluated with the HZETRN code with the appropriate database. In the current version of the code, the breakup of the primary ions and the knockout of target constituents by the neutrons and light ions are represented. Transition effects at the interface of dissimilar materials due to the atomic collisional nonequilibria (ref. 18) and neutron transition effects (ref. 19) are included in the present codes. Target fragmentation in each medium is represented by the equilibrium solution wherein transition effects near boundaries of dissimilar materials are neglected. Also neglected in the present calculations are the knockout of target constituents by multiple charged ions, pion production and transport, and coupling of the neutral pion field to the electromagnetic cascades. The addition of these processes to the transport codes further increases the dose behind a given thickness of shielding for which aluminum is perhaps an even less effective shield material than is indicated by the present calculation. Clearly, these issues need resolution before designing systems to send astronauts into space for extended periods.

GCR Radiation Protection From Various Thicknesses of Shielding

The annual dose and dose equivalent to critical body tissues during the 1977 solar minimum in a spherical shell of aluminum are shown in figure 4 and table 4. There is a transition effect in the skin and to a lesser extent in the ocular lens dose and dose equivalent as the

aluminum shield thickness is increased over the first few grams per square centimeter. No such transition is seen in the blood forming organ (BFO) since equilibrium is established in the surrounding tissue. The most constraining exposure limit is that for the BFO for which the 50 cSv/yr is not achieved until $\approx 30 \text{ g/cm}^2$. The LET distribution of the exposure is shown in figure 5 for three aluminum shield thicknesses. The main contribution to the dose equivalent is from particles with LET above 10 keV/ μm . The greatest attenuation of exposure is near 100 keV/ μm and above. This can be in part understood by observing figure 6 showing the contributions of various charge groups to dose equivalent. A large contribution comes from the iron ions ($Z = 26$) which can be broken up into smaller fragments by the shield. The iron ion has an associated LET of 200 keV/ μm and greater depending on the energy of the ion. The breakup of the ions results in a proliferation of light particles which attenuate more slowly in the shield material. Some of these light particles are produced as knockout particles from the shield nuclei and the control of the production of such light particles is part of the shielding problem. Considerable attenuation has already occurred in the transport of the radiation through body tissues in reaching the BFO. Shielding is therefore less effective in controlling the exposure. This effect can easily be seen in figure 6(b) since the BFO contribution from the iron ion is greatly reduced at even low shielding thicknesses (compare with ocular lens exposure in fig. 6(a)).

The various solar maxima were likewise different for different solar cycles, and the 1970 solar maximum resulted in the most intense minimum GCR environment observed over the last several solar cycles. The dose and dose equivalent for critical tissues are shown to attenuate slowly an aluminum spherical shell shield of varying thickness in figure 7 and table 5. This slow attenuation is distinct from the attenuation of the solar minimum environment where a great number of lower energy particles are present and are easily attenuated by low amounts of shielding with little contributions of secondary radiations. In distinction to figure 4, the dose at solar maximum in figure 7 increases dramatically due to secondary particle production processes in the aluminum shield. The increase is most dramatic for tissues near the body surface, whereas effects of secondary particle production processes are already apparent in the BFO which lies deeper in the human body. The aluminum shield is less effective in reducing the dose equivalent during solar maximum in all tissues as seen in figure 7(b).

From the results in figures 4 and 7, it is clear that aluminum is marginally useful as a shield material for reducing adverse astronaut health risks. In fact studies

using biological-based models of radiation response indicate that aluminum may indeed provide an additional hazard to the astronaut (ref. 7). This ineffectiveness and possibly added hazard of aluminum result from the secondary particle production processes in breaking up incident GCR ions within the shield. These effects can be reduced by introducing hydrogen into the shield as a chemical constituent. The possible use of polyethylene as a more efficient shield material is demonstrated for the 1977 solar minimum environment in figure 8. Again, a small transition effect is present in the first few millimeters of shielding in the skin dose which quickly disappears at the depth of the ocular lens. There is a persistent interface effect in crossing the polyethylene to tissue boundary which leaves the skin dose reduced relative to the ocular lens. This holds true also for the dose equivalent as seen in figure 8. This transition effect is caused by the equilibrium spectrum from atomic collisions which requires the particle stopping power times the flux (i.e., $S(E) \phi(E)$) to approach a constant at low energies. As $S(E)$ in the tissue and polyethylene differ, then the shape of the equilibrium spectrum is different, and the low-energy equilibrium spectrum in polyethylene is depleted in low-energy protons relative to equilibrium in tissue leaving the skin dose reduced. Equilibrium is reestablished within the tissue by the time the radiation reaches the ocular lens causing an increase in the dose. Whereas large amounts of aluminum were required to reduce the BFO dose equivalent to 50 cSv/yr, the polyethylene reduces the exposure of the BFO to this value in 10 g/cm². Note, the 10 g/cm² is less than the required 17 g/cm² for the dose at 5-cm depth which is often used to represent the BFO dose; this shows the importance of an accurate representation of the body geometry.

These improved attenuation characteristics of polyethylene shielding can be seen in the LET distribution of the organ exposures shown in figure 9. The reduction of dose equivalent occurs over the whole LET range as opposed to aluminum wherein the highest LET values were mainly affected. Clearly the attenuation of the highest LET is more efficient in the polyethylene, whereas secondary particle production is substantially lower in comparison with aluminum. These results are even better understood in terms of the charge distribution of the dose equivalent shown in figure 10. The heaviest ions are rapidly attenuated in the polyethylene with only modest increases of the single charged components and virtually no change in the double charged components. An important difference between aluminum and polyethylene is in the cluster knockout effects which were first observed in shuttle experiments (ref. 20). Clearly, a better knowledge of cluster effects in representing the nuclear structure is important to shield evaluation.

In addition to the GCR exposures, there is always the possibility of a major solar event. The solar events are random and unpredictable in both intensity and spectral content. The most important particles are protons in the energy range of 20 to 120 MeV (ref. 21). In the prior analysis of reference 21, we suggested that the design should be for the largest event observed which is on the order of the 97 percentile annual fluence and treat a possible larger event as an accidental exposure. Thus, the event on August 4, 1972, is the defining event. The dose and dose equivalent for this event are calculated according to measurements by the Interplanetary Monitoring Platform (IMP) satellite.

Crew Dosage Expected During Solar Proton Events on August 4, 1972

The HZETRN code and IMP satellite data have been used for the event on August 4, 1972, to evaluate the exposure of the astronaut critical tissues in a spherical shell shield of varying thickness. The results for an aluminum shell are in table 6. In a solar cycle independent design, the shield of approximately 30 g/cm² required for the 1977 solar minimum will be sufficient to give the required combined protection from both the 1970 solar maximum GCR environment and the August 4, 1972, event. However, the shield of 30 g/cm² would result in high mission cost. If a specific design for the solar maximum mission is considered, then a more modest shield of 10 g/cm² would be sufficient. Although a shield of 10 g/cm² is massive compared with those typical for space operations today, it may be considered manageable (ref. 16) but incompatible with the requirement of low mission cost.

If the aluminum can be replaced by a polyethylene shield, then the required shield of 10 g/cm² for a solar minimum will provide more than adequate protection from the combined environment of the August 4, 1972, event and the 1970 GCR environment. On the other hand, a polyethylene shield of about 7 g/cm² would provide adequate protection from both the 1970 GCR environment and the 1972 solar event. This thickness is still large compared with the shielding of a typical space station module but is comparable with the shield of 4.5 g/cm² used for the Apollo missions.

Radiation Protection Properties of Materials

The protection of the astronaut from space radiation is dependent on the local distribution of materials. Much of the protection will be derived from materials and equipment onboard the spacecraft for other purposes. The materials used to construct those systems would be of great importance and some attention needs to be given

to materials used in future spacecraft technology. It is clear from the present and past studies that the use of hydrogen-containing materials has great advantage over customary spacecraft materials. Design of water and food storage should likewise be utilized. Parasitic shielding is expensive, but polyethylene is a good material if added shield material is required. However, polyethylene has limited material properties and poses a flammability issue to be solved. Polymer composites are likely useful materials, but one would prefer a high binder-to-fiber ratio to maintain high hydrogen content. Careful consideration should be given to the other onboard materials.

The results in figure 2 show that, as particle production processes are added to the transport codes, the estimated attenuation properties show less protective properties. Aluminum is now estimated to be of little value in protection from the galactic cosmic rays, and further code improvement is expected to further detract from aluminum as a useful shield material. The increased importance of alternate materials will surely be the result of further code development. In this respect, a need exists to further identify potentially useful materials which are capable of providing the complete design properties required for spacecraft construction.

Concluding Remarks

Space radiation exposures will be the primary limiting factor in space exploration and in establishing a permanent human presence in space. During the past several years of shield code development, it has been established that aluminum space structures would make poor shields for human occupants. The need to look at new ways of constructing spacecraft is now evident because current estimates indicate aluminum to be an ineffective protection material. This result mainly comes from the secondary particle production processes in collision with target nuclei within the shield material and can be minimized by adding hydrogen as a constituent of the shield material. The most natural choice is polymeric materials for which advances in their development have been a focus for many years because of their mechanical properties. Their further development as a base construction material for future manned missions will have the added potential of minimizing the health risk to the astronaut from space radiations.

NASA Langley Research Center
Hampton, VA 23681-2199
September 16, 1997

References

1. Anon.: *NASA Strategic Plan*. NASA, Feb. 1996.
2. Schaefer, Hermann J.: Evaluation of Present-Day Knowledge of Cosmic Radiation at Extreme Altitude in Terms of the Hazard to Health. *J. Aviation Med.*, vol. 21, no. 5, Oct. 1950, pp. 375–394, 418.
3. Schimmerling, Walter: Radiobiological Problems in Space—An Overview. *Radiat. & Environ. Biophys.*, vol. 31, 1992, pp. 197–203.
4. National Council on Radiation Protection and Measurements: *Guidance on Radiation Received in Space Activities*. NCRP-98, July 1989.
5. Badhwar, G. D.; and O'Neill, P. M.: Galactic Cosmic Radiation Model and Its Applications. *Adv. Space Res.*, vol. 17, no. 2, 1996, pp. (2)7–(2)17.
6. Simonsen, Lisa C.; Nealy, John E.; and Townsend, Lawrence W.: *Concepts and Strategies for Lunar Base Radiation Protection—Prefabricated Versus In-Situ Materials*. SAE Paper 921370, July 1992.
7. Wilson, J. W.; Kim, M.-H.; Schimmerling, W.; Badavi, F. F.; Thibeault, S. A.; Cucinotta, F. A.; Shinn, J. L.; and Kieffer, R. L.: Issues in Space Radiation Protection: Galactic Cosmic Rays. *Health Phys.*, vol. 68, no. 1, Jan. 1995, pp. 50–58.
8. Letaw, J. R.; Silberberg, R.; and Tsao, C. H.: Radiation Hazards on Space Missions Outside the Magnetosphere. *Adv. Space Res.*, vol. 9, no. 10, 1989, pp. 285–291.
9. Wilson, John W.; Townsend, Lawrence W.; and Badavi, F. F.: A Semiempirical Nuclear Fragmentation Model. *Nucl. Instrum. & Methods Phys. Res.*, vol. B18, no. 3, Feb. 1987, pp. 225–231.
10. Wilson, J. W.; Townsend, L. W.; and Badavi, F. F.: Galactic HZE Propagation Through the Earth's Atmosphere. *Radiat. Res.*, vol. 109, no. 2, 1987, pp. 173–183.
11. Townsend, Lawrence W.; Cucinotta, Francis A.; and Wilson, John W.: HZE Reactions and Data-Base Development. *Biological Effects and Physics of Solar and Galactic Cosmic Radiation*, Part B, Charles E. Swenberg, Gerda Horneck, and E. G. Stassinopoulos, eds., Plenum Press, 1993, pp. 787–809.
12. Shinn, J. L.; Wilson, J. W.; Badavi, F. F.; Benton, E. V.; Csige, I.; Frank, A. L.; and Benton, E. R.: HZE Beam Transport in Multilayered Materials. *Radiat. Meas.*, vol. 23, no. 1, Jan. 1994, pp. 57–64.
13. Wilson, J. W.; Tripathi, R. K.; Cucinotta, F. A.; Shinn, J. L.; Badavi, F. F.; Chun, S. Y.; Norbury, J. W.; Zeitlin, C. J.; Heilbronn, L.; and Miller, J.: *NUCFRG2: An Evaluation of the Semiempirical Nuclear Fragmentation Database*. NASA TP-3533, 1995.
14. Cucinotta, F. A.; Townsend, L. W.; Wilson, J. W.; Shinn, J. L.; Badhwar, G. D.; and Dubey, R. R.: Light Ion Components of the Galactic Cosmic Rays: Nuclear Interactions and Transport Theory. *Adv. Space Res.*, vol. 17, no. 2, 1996, pp. (2)77–(2)86.
15. Wilson, John W.; Nealy, John E.; Schimmerling, Walter; Cucinotta, Francis A.; and Wood, James S.: *Effects of Radiobiological Uncertainty on Vehicle and Habitat Shield Design for Missions to the Moon and Mars*. NASA TP-3312, 1993.
16. Nealy, John E.; Striepe, Scott A.; and Simonsen, Lisa C.: *MIRACAL: A Mission Radiation Calculation Program for Analysis of Lunar and Interplanetary Missions*. NASA TP-3211, 1992.
17. Atwell, William; Weyland, Mark D.; and Simonsen, Lisa C.: Solar Particle Dose Rate Buildup and Distribution in Critical Body Organs. *Biological Effects and Physics of Solar and Galactic Cosmic Radiation*. Part B, Charles E. Swenberg, Gerda Horneck, and E. G. Stassinopoulos, eds., Plenum Press, 1993, pp. 831–844.
18. Wilson, John W.; and Badavi, Francis F.: *A Study of the Generation of Linear Energy Transfer Spectra for Space Radiations*. NASA TM-4410, 1992.
19. Lamkin, S. L.; Khandelwal, G. S.; Shinn, J. L.; and Wilson, J. W.: Space Proton Transport in One Dimension. *Nucl. Sci. & Eng.*, vol. 116, no. 4, Apr. 1994, pp. 291–299.
20. Badhwar, G. D.; Patel, J. U.; Cucinotta, F. A.; and Wilson, J. W.: Measurements of the Secondary Particle Energy Spectra in the Space Shuttle. *Radiat. Meas.*, vol. 24, no. 2, Apr. 1995, pp. 129–138.
21. Wilson, John W.; Shinn, Judy L.; Simonsen, Lisa C.; Cucinotta, Francis A.; Dubey, R. R.; Jordan, W. R.; Jones, T. D.; Chang, C. K.; and Kim, M. Y.: *Exposures to Solar Particle Events in Deep Space Missions*. NASA TP-3668, 1997.

Table 1. Ionizing Radiation Exposure Limits

[From NCRP 98 (ref. 4)]

Exposure interval	Dose equivalent, Sv, for—		
	Blood forming organ (BFO)	Skin	Ocular lens
Career	^a 1–4	6	4
Annual	0.5	3	2
30 Days	0.25	1.5	1

^aVaries with age and gender at initial exposure.

Table 2. Annual Dose and Dose Equivalent for GCR in Spherical Shell Shield for 1977 Solar Minimum

Shielding thickness, x , g/cm ²	Dose, D , cGy/yr, for depth of—		Dose equivalent, H , cSv/yr, for depth of—	
	0 cm	5 cm	0 cm	5 cm
Aluminum				
0	19	20	120	95
1	22	20	132	91
2	22	20	127	88
5	22	20	111	79
10	22	20	93	69
25	21	19	69	54
50	19	18	56	46
75	18	17	53	43
Polyethylene				
0	19	20	120	95
1	21	20	118	89
2	20	20	109	83
5	20	19	87	71
10	19	19	64	57
25	17	17	39	41
50	16	16	31	35
75	14	14	28	32

Table 3. Annual Dose and Dose Equivalent for GCR in Spherical Shell Shield for 1970 Solar Maximum

Shielding thickness, x , g/cm ²	Dose, D , cGy/yr, for depth of—		Dose equivalent, H , cSv/yr, for depth of—	
	0 cm	5 cm	0 cm	5 cm
Aluminum				
0	6.1	6.9	37.9	34.5
1	7.2	7.0	39.1	33.7
2	7.4	7.0	37.0	32.9
5	7.7	7.1	31.4	30.7
10	7.9	7.2	24.5	27.8
25	8.0	7.4	15.4	22.8
50	7.9	7.4	12.4	20.0
75	7.7	7.3	11.7	19.4
Polyethylene				
0	6.1	6.9	37.9	34.5
1	6.6	6.9	39.1	32.7
2	6.7	6.9	37.1	31.2
5	6.7	6.8	31.4	27.2
10	6.5	6.7	24.5	22.6
25	6.2	6.4	15.3	16.4
50	6.0	6.2	12.3	14.4
75	5.8	5.8	11.7	13.7

Table 4. Annual Dose and Dose Equivalent for GCR Behind Slab Shield for 1977 Solar Minimum

Shielding thickness, x , g/cm ²	Dose, D , cGy/yr, to—			Dose equivalent, H , cSv/yr, to—		
	Skin	Ocular lens	BFO	Skin	Ocular lens	BFO
Aluminum						
0.00	19.66	20.44	19.52	96.09	104.31	73.13
0.30	20.33	20.33	19.53	100.69	100.08	72.56
1.00	20.60	20.43	19.50	98.78	97.46	71.17
3.00	20.75	20.50	19.43	92.11	90.46	67.67
5.00	20.74	20.47	19.36	86.29	84.55	64.69
10.00	20.57	20.30	19.20	75.37	73.51	58.90
20.00	20.14	19.89	18.86	62.66	60.67	51.76
30.00	19.69	19.46	18.51	55.93	53.92	47.84
50.00	18.76	18.57	17.75	49.69	47.79	44.07
Polyethylene						
0.00	19.66	20.44	19.52	96.09	104.31	73.13
0.30	19.96	20.27	19.48	96.69	99.47	72.01
1.00	19.93	20.17	19.35	92.17	94.69	69.47
3.00	19.58	19.79	19.02	80.64	83.04	63.33
5.00	19.22	19.42	18.74	71.71	74.06	58.43
10.00	18.49	18.68	18.17	56.84	59.09	49.90
20.00	17.52	17.71	17.34	42.95	45.12	41.40
30.00	16.84	17.03	16.68	37.45	39.63	37.75
50.00	15.68	15.86	15.47	33.38	35.60	34.52

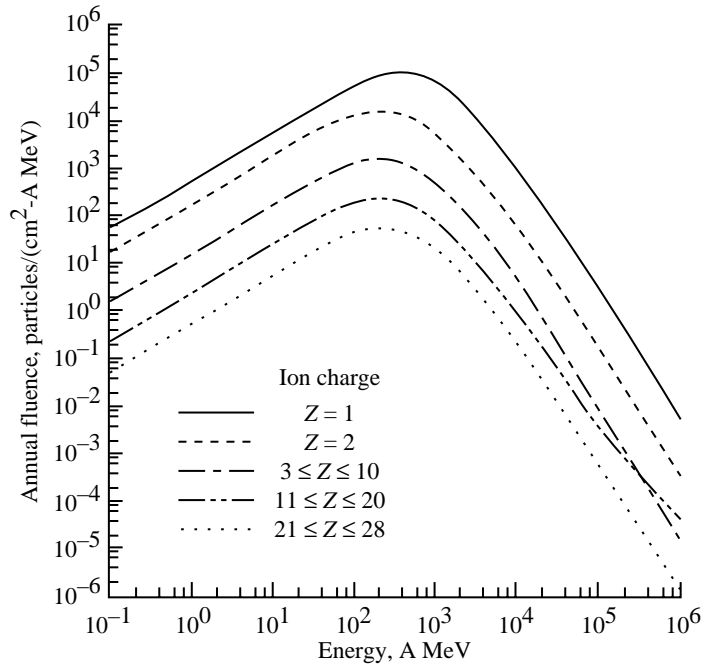
Table 5. Annual Dose and Dose Equivalent for GCR Behind Slab Shield for 1970 Solar Maximum

Shielding thickness, x , g/cm ²	Dose, D , cGy/yr, to—			Dose equivalent, H , cSv/yr, to—		
	Skin	Ocular lens	BFO	Skin	Ocular lens	BFO
Aluminum						
0.00	6.55	6.76	6.82	32.67	34.80	27.65
0.30	6.85	6.84	6.83	34.87	34.77	27.49
1.00	7.03	6.96	6.86	34.78	34.44	27.17
3.00	7.25	7.15	6.94	33.70	33.20	26.33
5.00	7.37	7.26	7.00	32.51	31.95	25.56
10.00	7.54	7.43	7.10	29.88	29.24	23.95
20.00	7.69	7.59	7.23	26.22	25.50	21.77
30.00	7.75	7.65	7.29	24.05	23.29	20.52
50.00	7.72	7.64	7.31	21.99	21.23	19.41
Polyethylene						
0.00	6.55	6.76	6.82	32.67	34.80	27.65
0.30	6.69	6.79	6.81	33.37	34.43	27.28
1.00	6.74	6.82	6.79	32.41	33.37	26.52
3.00	6.74	6.80	6.75	29.50	30.39	24.57
5.00	6.70	6.76	6.70	26.94	27.79	22.92
10.00	6.57	6.63	6.59	22.15	22.95	19.87
20.00	6.39	6.45	6.44	17.07	17.84	16.63
30.00	6.28	6.34	6.33	14.96	15.73	15.26
50.00	6.09	6.15	6.10	13.60	14.40	14.28

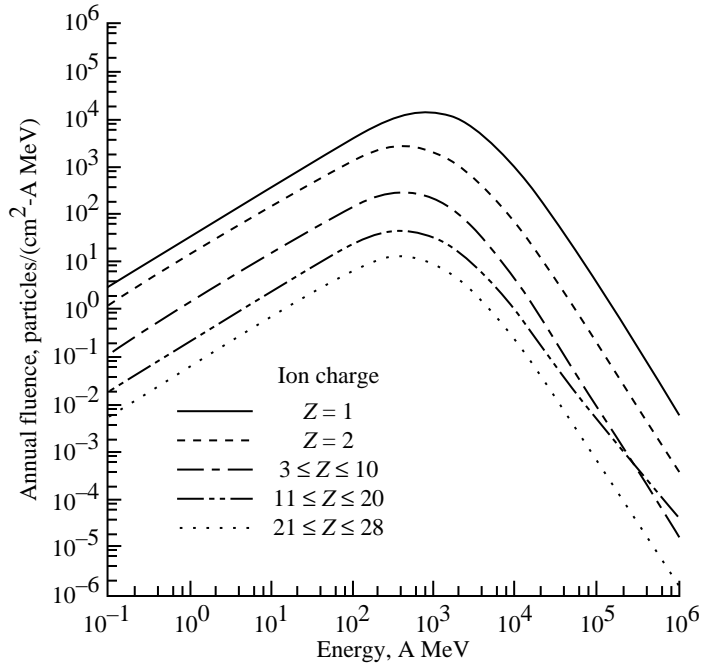
Table 6. Dose and Dose Equivalent Behind Shield for Solar Event on August 4, 1972

[Data from IMP satellite]

Shielding thickness, x , g/cm ²	Skin		Ocular lens		BFO	
	Dose, D , cGy	Dose equivalent, H , cSv	Dose, D , cGy	Dose equivalent, H , cSv	Dose, D , cGy	Dose equivalent, H , cSv
Aluminum						
0.4	4830	9350	2400	3830	157	217
1	2120	3560	1420	2140	130	180
5	294	427	263	367	46.9	65
10	76.1	110.01	71.4	101.01	16.7	24.3
25	10.4	16.8	10.2	16.8	3.23	5.85
50	0.313	1.34	0.378	1.66	0.216	0.891
Polyethylene						
0.4	3620.01	6770.01	2080.01	3530.01	151.01	221.01
1	1540.01	2510.01	1150.01	1810.01	120.01	174.01
5	184.01	267.01	171.01	251.01	34.2	50.01
10	39.4	58.01	38.01	56.9	9.98	15.5
25	1.68	3.45	1.71	3.68	0.69	1.7
50	0.12	0.49	0.13	0.54	0.09	0.35



(a) GCR ion fluence for 1977 solar minimum.



(b) GCR ion fluence for 1981 solar maximum.

Figure 1. Differential annual fluence spectra.

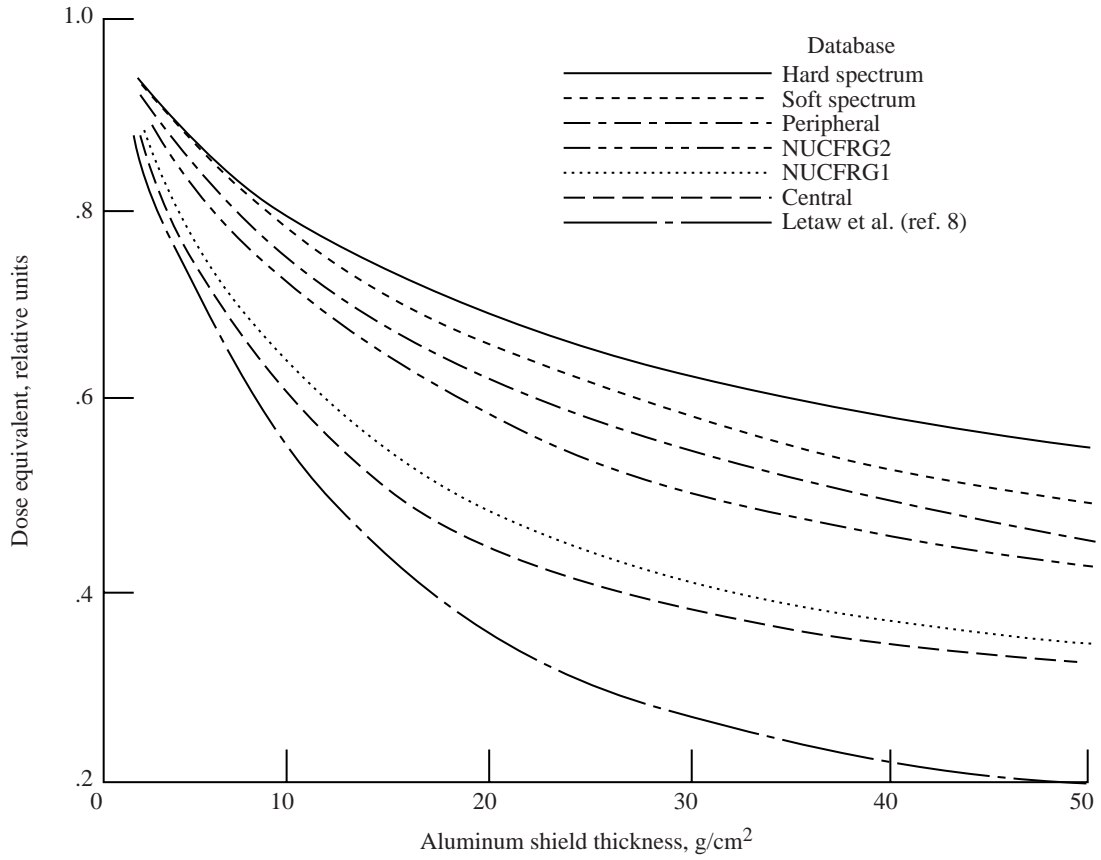


Figure 2. Shield attenuation for solar minimum GCR dose equivalent resulting from nuclear fragmentation models.

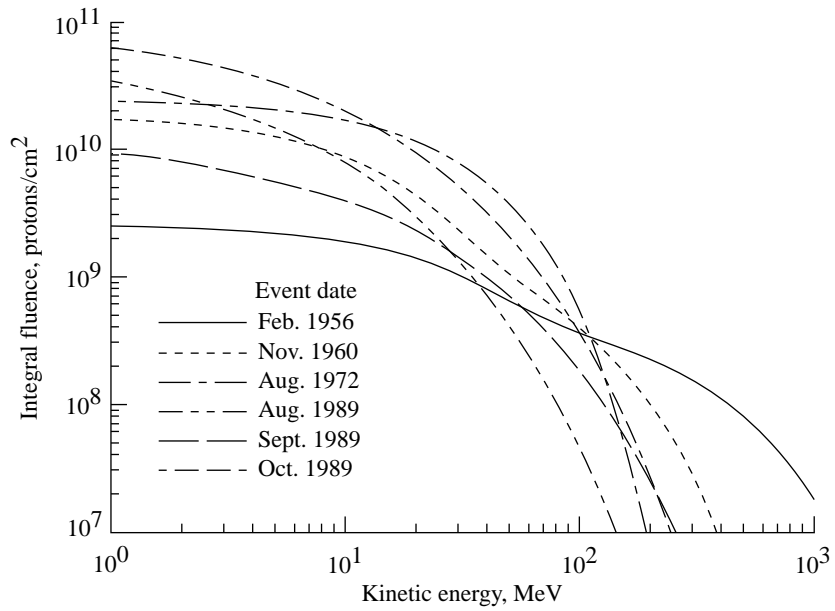
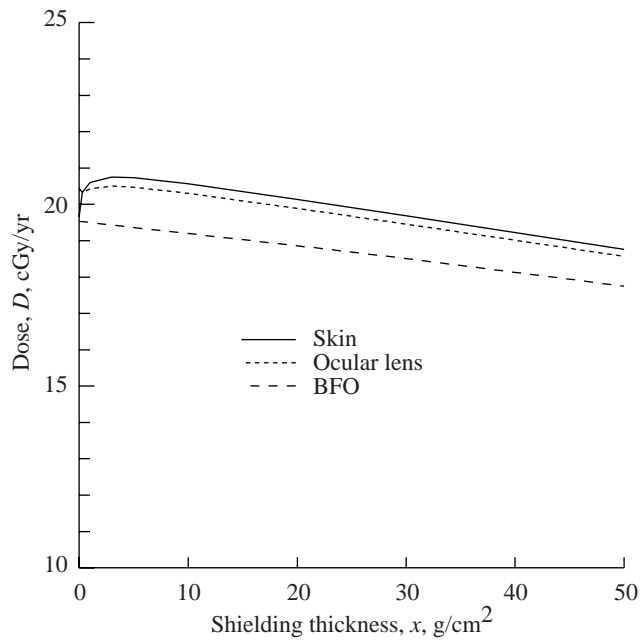
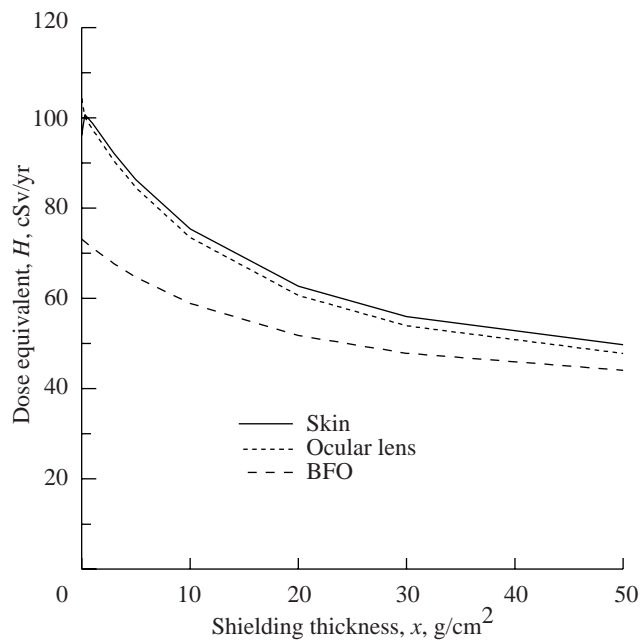


Figure 3. Large solar proton event spectra at 1 AU.

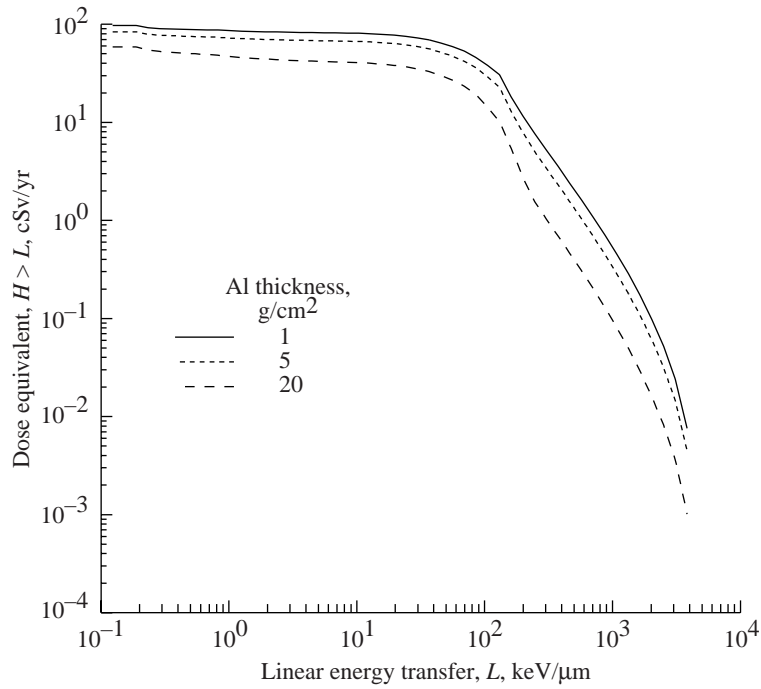


(a) Dose.

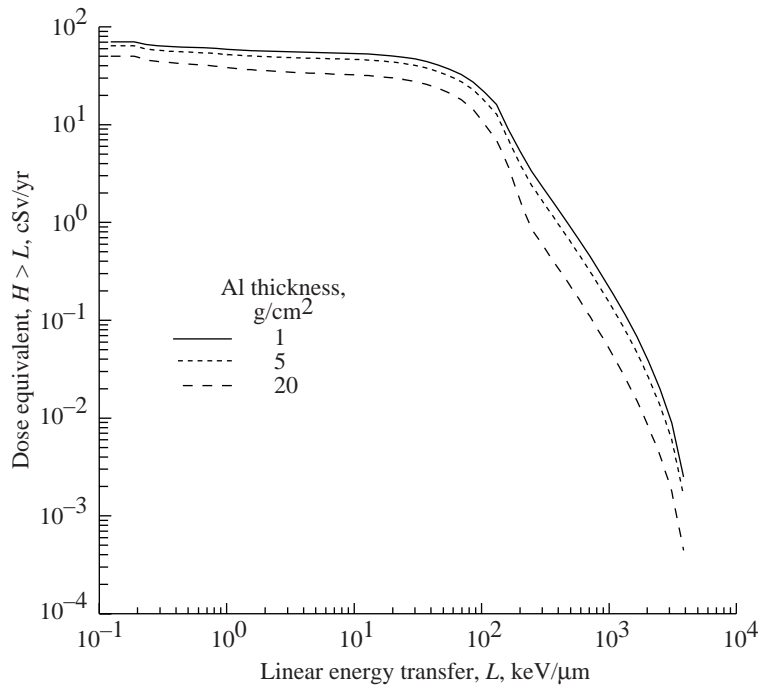


(b) Dose equivalent.

Figure 4. Annual GCR dose and dose equivalent during 1977 solar minimum behind aluminum shielding of varying thickness.

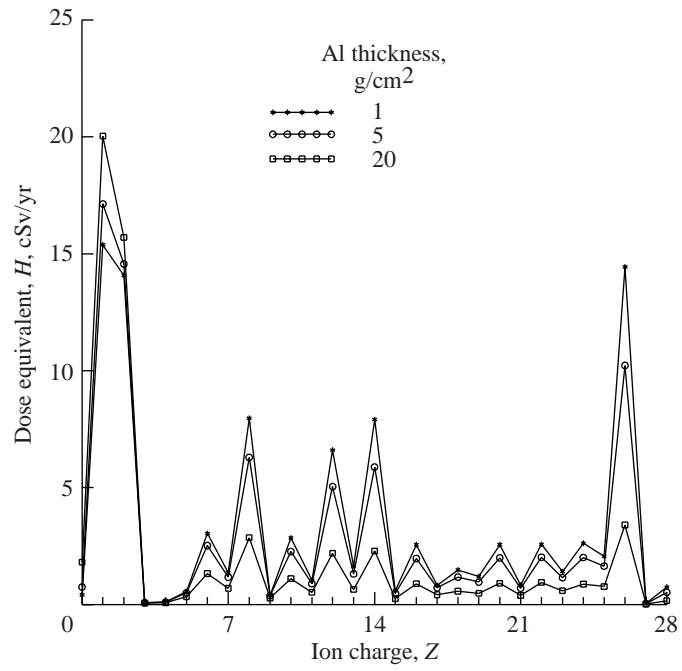


(a) Ocular lens.

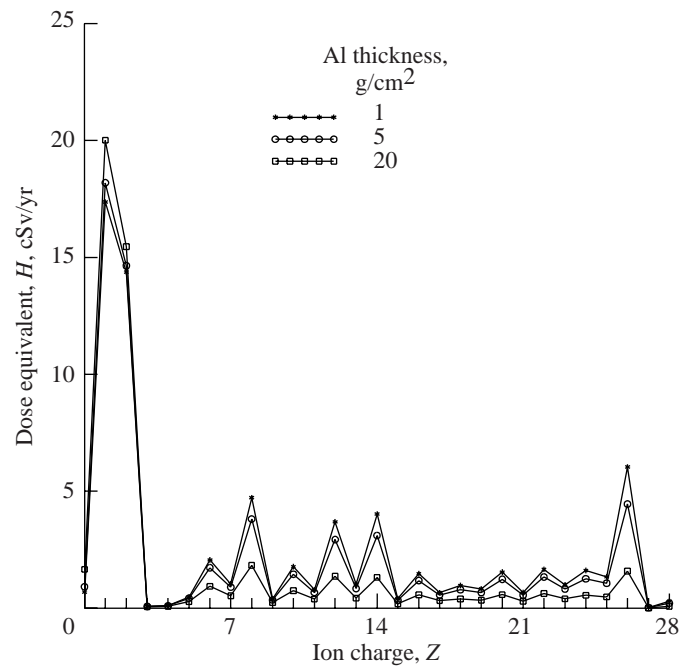


(b) BFO.

Figure 5. Distribution of dose equivalent to ocular lens and BFO over LET behind various amounts of aluminum shielding for 1977 solar minimum.

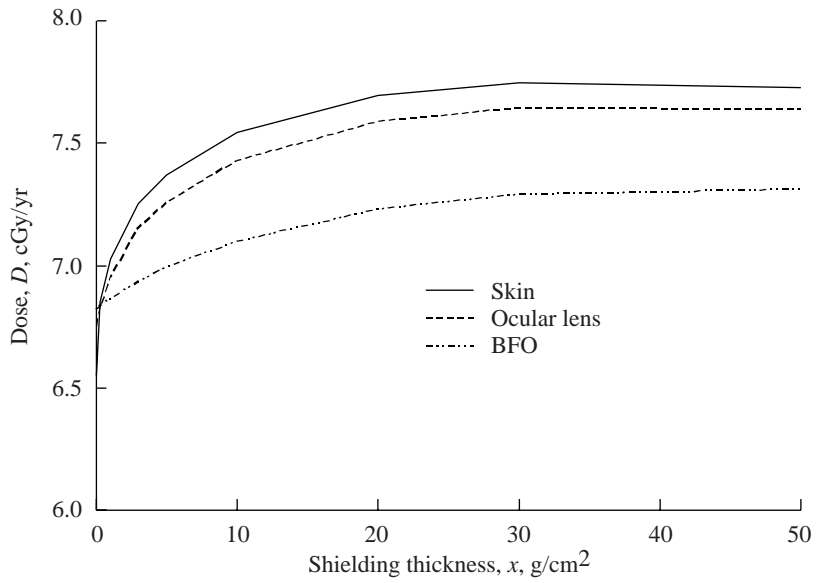


(a) Ocular lens.

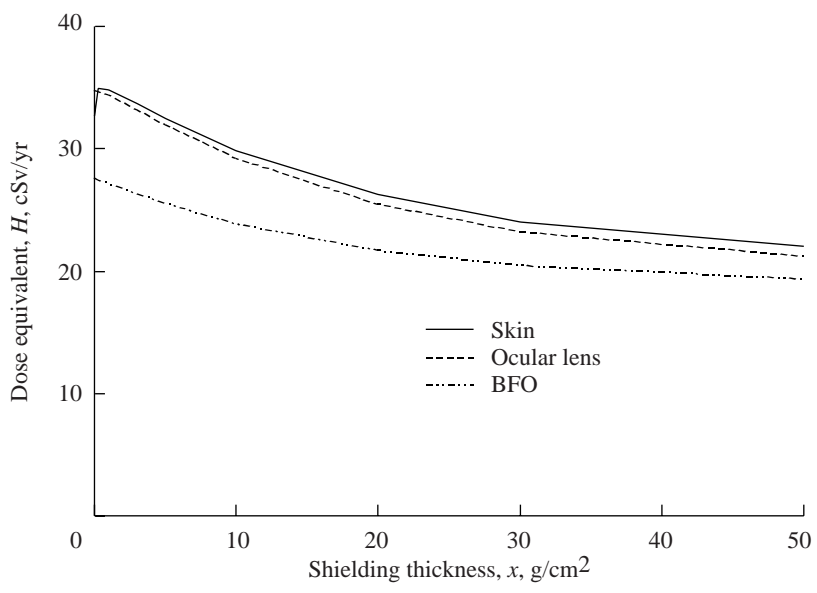


(b) BFO.

Figure 6. Distribution of dose equivalent to ocular lens and BFO over ion charge behind various amounts of aluminum shielding for 1977 solar minimum.

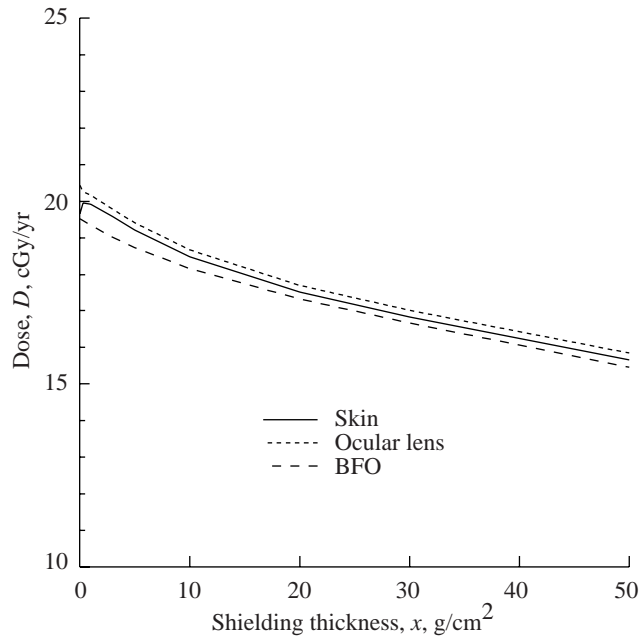


(a) Dose.

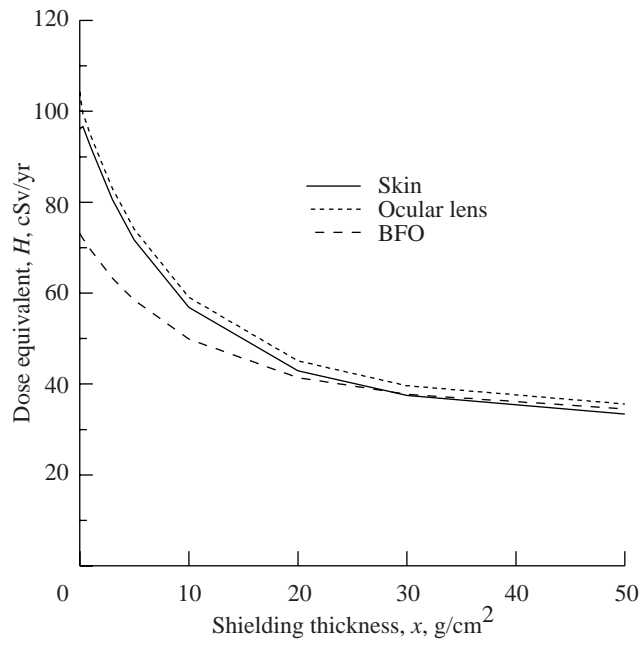


(b) Dose equivalent.

Figure 7. Annual GCR dose and dose equivalent during 1970 solar maximum behind aluminum shielding of varying thickness.

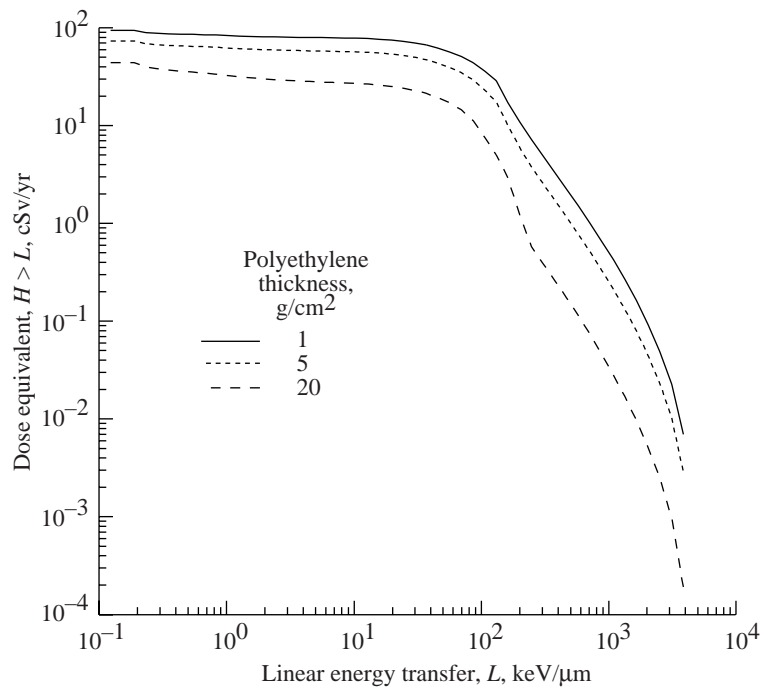


(a) Dose.

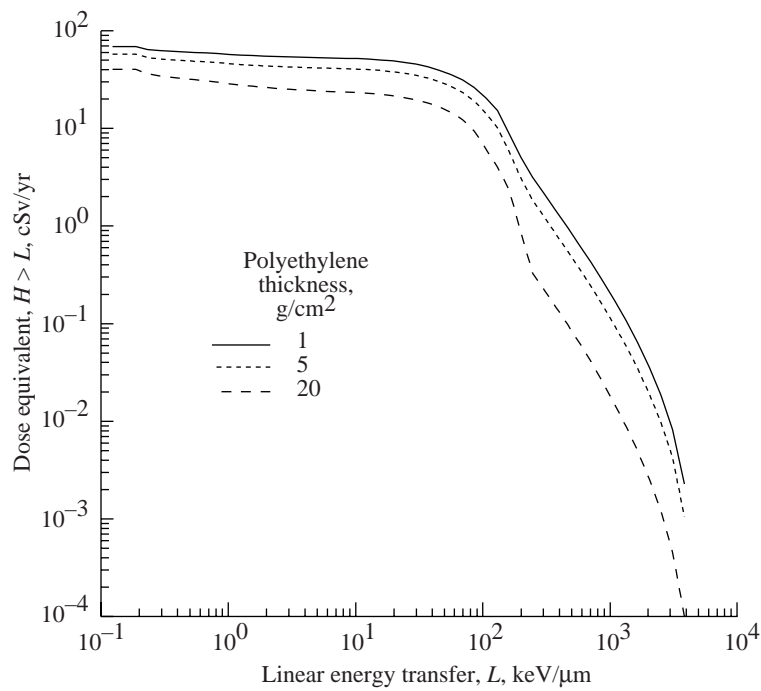


(b) Dose equivalent.

Figure 8. Annual GCR dose and dose equivalent during 1977 solar minimum behind polyethylene shielding of varying thickness.

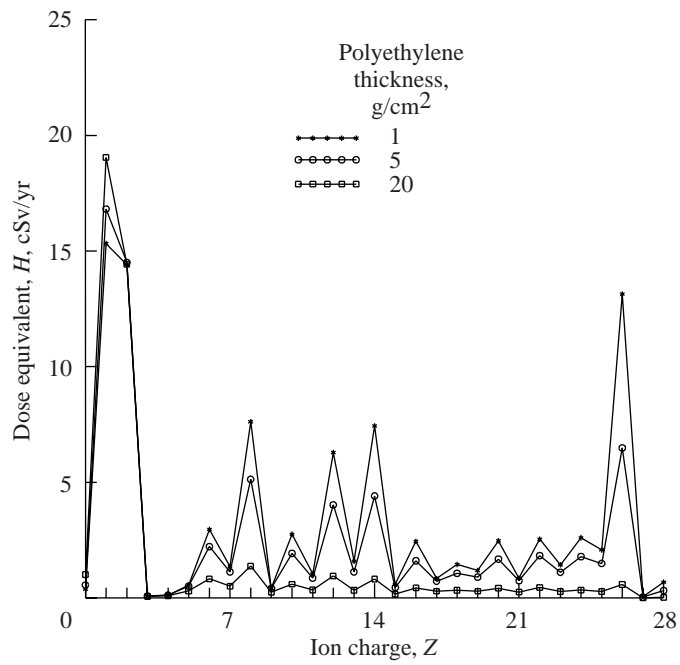


(a) Ocular lens.

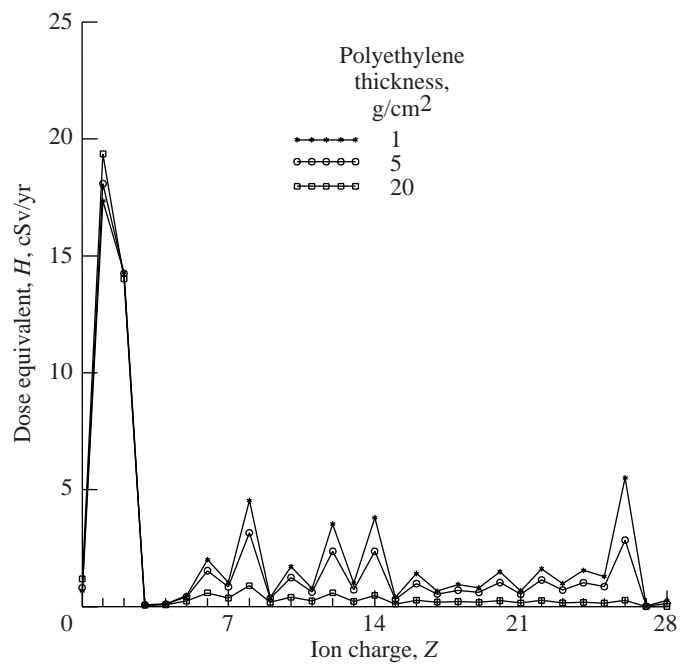


(b) BFO.

Figure 9. Distribution of dose equivalent to ocular lens and BFO over LET behind various amounts of polyethylene shielding for 1977 solar minimum.



(a) Ocular lens.



(b) BFO.

Figure 10. Distribution of dose equivalent to ocular lens and BFO over ion charge behind various amounts of polyethylene shielding for 1977 solar minimum.

REPORT DOCUMENTATION PAGE

Form Approved
OMB No. 0704-0188

Public reporting burden for this collection of information is estimated to average 1 hour per response, including the time for reviewing instructions, searching existing data sources, gathering and maintaining the data needed, and completing and reviewing the collection of information. Send comments regarding this burden estimate or any other aspect of this collection of information, including suggestions for reducing this burden, to Washington Headquarters Services, Directorate for Information Operations and Reports, 1215 Jefferson Davis Highway, Suite 1204, Arlington, VA 22202-4302, and to the Office of Management and Budget, Paperwork Reduction Project (0704-0188), Washington, DC 20503.

1. AGENCY USE ONLY <i>(Leave blank)</i>		2. REPORT DATE December 1997	3. REPORT TYPE AND DATES COVERED Technical Paper	
4. TITLE AND SUBTITLE Galactic and Solar Cosmic Ray Shielding in Deep Space			5. FUNDING NUMBERS WU 199-45-16-11	
6. AUTHOR(S) John W. Wilson, Francis A. Cucinotta, H. Tai, Lisa C. Simonsen, Judy L. Shinn, Shelia A. Thibeault, and M. Y. Kim				
7. PERFORMING ORGANIZATION NAME(S) AND ADDRESS(ES) NASA Langley Research Center Hampton, VA 23681-2199			8. PERFORMING ORGANIZATION REPORT NUMBER L-17634	
9. SPONSORING/MONITORING AGENCY NAME(S) AND ADDRESS(ES) National Aeronautics and Space Administration Washington, DC 20546-0001			10. SPONSORING/MONITORING AGENCY REPORT NUMBER NASA TP-3682	
11. SUPPLEMENTARY NOTES Wilson, Cucinotta, Tai, Simonsen, Shinn, and Thibeault: Langley Research Center, Hampton, VA; Kim: NRC-Resident Research Associate at Langley Research Center, Hampton, VA.				
12a. DISTRIBUTION/AVAILABILITY STATEMENT Unclassified-Unlimited Subject Category 92 Availability: NASA CASI (301) 621-0390			12b. DISTRIBUTION CODE	
13. ABSTRACT <i>(Maximum 200 words)</i> An analysis of the radiation hazards in support of NASA deep space exploration activities is presented. The emphasis is on materials required for radiation protection shielding. Aluminum has been found to be a poor shield material when dose equivalent is used with exposure limits for low Earth orbit (LEO) as a guide for shield requirements. Because the radiation issues are cost related—the parasitic shield mass has high launch costs—the use of aluminum as a basic construction material is clearly not cost-effective and alternate materials need to be developed. In this context, polyethylene is examined as a potentially useful material and demonstrates important advantages as an alternative to aluminum construction. Although polyethylene is useful as a shield material, it may not meet other design criteria (strength, stability, thermal); other polymer materials must be examined.				
14. SUBJECT TERMS Solar events; Cosmic rays; Shielding			15. NUMBER OF PAGES 22	
			16. PRICE CODE A03	
17. SECURITY CLASSIFICATION OF REPORT Unclassified	18. SECURITY CLASSIFICATION OF THIS PAGE Unclassified	19. SECURITY CLASSIFICATION OF ABSTRACT Unclassified	20. LIMITATION OF ABSTRACT	